PERGAMON

International Journal of Solids and Structures 38 (2001) 1889–1902

INTERNATIONAL JOURNAL OF SOLIDS and STRUCTURES

www.elsevier.com/locate/ijsolstr

Friction and rigid body identification of robot dynamics

M. Grotjahn *,[1], M. Daemi, B. Heimann *,[2]

Institute of Mechanics, University of Hanover, Appelstrasse 11, D-30167 Hanover, Germany

Received 3 September 1999; in revised form 29 December 1999

Abstract

In this paper, an identification method for industrial robots is described that does not require the a priori identification of the friction model. First, the necessity for such a method is motivated by an overview on conventional friction modelling and rigid body identification. It is shown that the time variance of typical friction characteristics lead to systematic identification errors. They are avoided by the presented method, which is based on separating the base parameters into three different groups. Each group is identified by simple measurements and a weighted *least-squares* method. Measurements are carried out with simple motions in the neighbourhood of a number of especially selected joint configurations. Further advantages of this method are its easy implementation for standard robot controls and the possibility to find modelling errors. The experimental implementation of this method to a typical industrial robot with six rotational joints is carried out and yields remarkable results.

Keywords: Industrial robot; Modelling; Identification; Dynamics; Friction

1. Introduction

Common identification methods for industrial robots are based on the description of the equation of motion in terms of a linear parameter vector of minimal order (base parameters) (Gautier and Khalil, 1988a; Khosla, 1988) and the use of *least-squares* (LS) error minimisation criteria (Armstrong, 1988, 1989; Daemi and Heimann, 1996; Daemi and Grotjahn, 1996; Gautier and Khalil, 1988b; Gautier et al., 1995; Lawson and Hanson, 1974; Pfeiffer and Hölzl, 1995; Presse and Gautier, 1993; Prüfer et al., 1994). The robot is typically moved along a trajectory, which is generated using an optimisation scheme to attain maximum excitation of all base parameters. Joint motion and joint torque are measured and the torque due to friction is compensated using a measured friction model. Then, a batch LS algorithm is used to calculate the base parameter vector.

In practice, it can be observed that, even with good excitation of all parameters, the results still show some systematic errors (Daemi and Heimann, 1996; Daemi and Grotjahn, 1996). One reason for these

* Corresponding authors.

E-mail addresses: grotjahn@ifm.uni-hannover.de (M. Grotjahn), heimann@ifm.uni-hannover.de (B. Heimann).

[1] Fax: +49-511-762-7010179.

[2] Tel.: +49-511-762-4161; fax: +49-511-762-4164.

0020-7683/01/$ - see front matter
PII: S0020-7683(00)00141-4

errors is the variation of friction characteristics during the measurements. Further difficulties arise from the restrictions of standard robot controls, since optimised trajectories usually require additional hardware for generating arbitrary joint motions.

In this paper, a two-step approach for the identification of the base parameter vector is described. It is an extension of the algorithm introduced by Seeger (1992) which requires only trajectories with trapezoidal velocity characteristic and no a priori compensation of the friction model. The idea is to measure directly the moments of inertia and the gravitational torques for a number of different joint configurations. The resulting values are used to calculate the base parameter vector by a weighted LS method. The only assumption that has to be verified in advance is that the friction characteristics are symmetric.

The modelling and the time variance of friction are discussed in Sections 2 and 3. In Section 4, the rigid body modelling is presented. Section 5 gives an overview on conventional identification methods. The two-step identification scheme is explained in Section 6. And finally, in Sections 7 and 8, the experimental set-up and results are depicted. The results hold for a wide range of industrial robots, since the tested manipulator *Siemens manutec-r15* is a typical industrial system with different types of gears.

2. Modelling and identification of gear friction

Normally, very stiff gears with small backlash are used in industrial robotics. Therefore, gear elasticity and backlash have small influence on the controlled system's dynamics. This influence can be avoided by a proper choice of identification measurements.

Besides rigid body dynamics, only the losses in gears and bearings are taken into account by friction models. For their identification, friction has to be separated from other dynamic effects. By using trajectories, where only one axis is moved, and selecting parts of the measurement with constant velocity, the influences of acceleration, centrifugal and Coriolis forces are eliminated. If gravitation has an influence on the torque of the regarded axis, it has to be compensated by a model identified in advance. Thus, the following measurements can be assumed to solely reflect the influence of friction in gears and bearings. The identification of gravitation model can be done without the knowledge about friction behaviour by the method proposed in Section 6.

Friction losses of a single robotic joint i are usually modelled as a torque $Q_{i,\mathrm{f1}}$ which is a function of its own rotational joint speed $\dot{q}_i$. This non-linear function is mostly described by the sum of terms for viscous damping and dry friction (Armstrong-Hélouvry, 1991; Armstrong-Hélouvry et al., 1994; Canudas de Wit et al., 1991; Pfeiffer and Hölzl, 1995; Seeger, 1992):

$$Q_{i,\mathrm{f1}} = a_{i,1}\dot{q}_i + a_{i,2}\mathrm{sign}(\dot{q}_i). \tag{1}$$

This simple model needs to be refined for more precise modelling (Daemi and Heimann, 1996; Prüfer and Wahl, 1994). Fig. 1a shows measured friction torques of some axes of a robot over their full speed range, normalised to their maximum speed and maximum torque. It can be seen that all axes show significant degressive characteristics, not covered by the simple model given in Eq. (1). A better description of the measured friction characteristics can be found by using one of the following equations:

$$Q_{i,\mathrm{f2}} = a_{i,1}\dot{q}_i + a_{i,2}\mathrm{sign}(\dot{q}_i) + a_{i,3}\dot{q}_i^{1/3}, \tag{2}$$

$$Q_{i,\mathrm{f3}} = a_{i,1}\dot{q}_i + a_{i,2}\mathrm{sign}(\dot{q}_i) + a_{i,3}\,\mathrm{atan}(a_{i,4}\dot{q}_i). \tag{3}$$

For a given measured friction characteristic, an analytical description with a minimal square model error can easily be calculated for Eqs. (1) and (2), since they have only linear dependencies with respect to their parameters. Whereas for model (3), a non-linear optimisation procedure is applied. As depicted in Fig. 1b, both models lead to much better results than the classic equation (1). The mean quadratic error between the

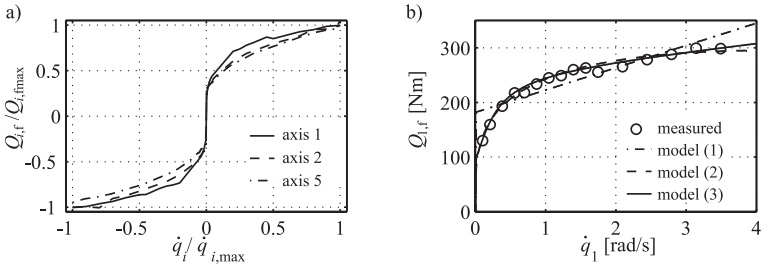

Fig. 1. (a) Normalised friction characteristics for different axes of the *manutec-r15*. (b) Adaption of friction models to measured friction characteristics of axis 1.

measured and modelled torque is used to decide whether model (2) or (3) gives a better description of the measured characteristics. It has to be kept in mind that modelled parameters a_j found in this way no longer represent mechanical models (such as dry friction or viscous damping) but merely force the sum of all effects of the multistage gears into a mathematical description.

3. Time variance of friction characteristics

The major problem in friction modelling is the time variance of friction (Daemi and Heimann, 1996, 1998; Prüfer and Wahl, 1994). Commonly, relatively large time constants are assumed that arise from temperature variation in gears and bearings. Thus, the typical approach for the friction modelling in robotics is to use some 'warm-up' time, where the robot is supposed to reach stationary conditions (Armstrong, 1991; Daemi and Heimann, 1996; Seeger, 1992). The measurements in Fig. 2a shows that this does not generally hold for geared robots.

The figure shows friction with respect to time for a multistage robot gear which is continuously moved back and forth. The torque is measured every 12 s in periods, with constant velocity. The motion is interrupted at different times for short periods (5, 1 and 2 min). It shows that after these short interruptions, the friction becomes significantly larger. This effect implies that not only temperature but also the distribution of lubricants determines friction conditions. Therefore, it is very difficult to ensure equal conditions for the friction characteristics at two separate measurements. Actually, even during a precise friction measurement (which takes a few minutes) operating conditions might change.

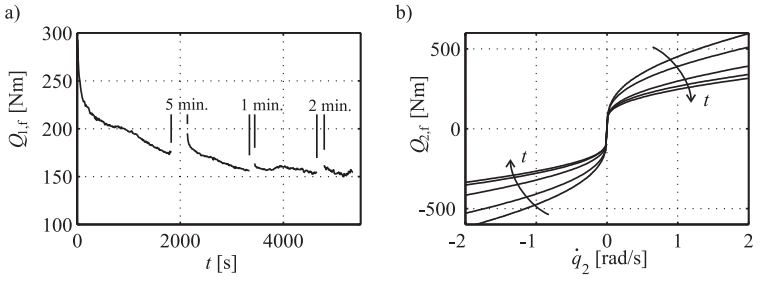

Fig. 2. Time variance of friction characteristics: (a) variations during steadily back and forth motion with short brakes, and (b) change of friction characteristic of joint 2 during continuous operation.

The changing of measured friction characteristics is depicted in Fig. 2b. Even with changing friction characteristic, the graphs stay almost symmetric. This behaviour was observed for a number of different types of robot gears, although different experiences are described in the literature (Armstrong, 1988; Pfeiffer and Hölzl, 1995). But since a symmetric friction characteristic is essential for the proposed identification method, it should be verified if necessary.

4. Parameter-linear modelling of rigid body dynamics

For identification, a representation of robot dynamics has to be determined which is linear with respect to the unknown inertial and gravitational parameters. In this section, the basic idea for this determination is described. It is derived using the modified *Denavit–Hartenberg* (MDH) notation for robot kinematics (Khalil and Kleinfinger, 1986). The resulting base parameter vector is grouped according to the requirements of the identification scheme shown in Section 6.

4.1. Dynamic parameters

The dynamic parameters of each link i consist of its mass m_i, its first moment $\boldsymbol{s}_i := [\, s_{xi} \quad s_{yi} \quad s_{zi} \,]^{\mathrm{T}} = m_i \boldsymbol{r}^i_{\mathrm{Ci}}$ ($\boldsymbol{r}^i_{\mathrm{Ci}}$ is the vector from the link's coordinate frame to its centre of mass) and its inertia tensor about the corresponding coordinate frame $\boldsymbol{I}_i^{(i)}$. Collecting the independent scalar components of $\boldsymbol{s}_i$ and $\boldsymbol{I}_i^{(i)}$ results in the parameter vector,

$$\boldsymbol{p}_{\mathrm{link},i} = [\, I_{xxi} \quad I_{xyi} \quad I_{xzi} \quad I_{yyi} \quad I_{yzi} \quad I_{zzi} \quad s_{xi} \quad s_{yi} \quad s_{zi} \quad m_i \,]^{\mathrm{T}}, \tag{4}$$

which leads to the over-all parameter vector,

$$\boldsymbol{p} = \left[\boldsymbol{p}_{\mathrm{link},1}\ \boldsymbol{p}_{\mathrm{link},2}\ \cdots\ \boldsymbol{p}_{\mathrm{link},n}\right]^{\mathrm{T}}. \tag{5}$$

In practical robotic applications, a number of parameters are zero because of the orientation and position of the coordinate frames as well as symmetric shapes of the bodies. Furthermore, a large number of parameters can be replaced by linear combinations (Section 4.3).

4.2. Equations of motions in parameter-linear form

The equations of motion of tree-structured robots can be derived in parameter-linear form by the *Newton–Euler* approach (Khosla, 1988) or the *Lagrangian equations of second kind* (Gautier and Khalil, 1988a):

$$\boldsymbol{Q} = \boldsymbol{M}(\boldsymbol{q})\ddot{\boldsymbol{q}} + \boldsymbol{c}(\boldsymbol{q}, \dot{\boldsymbol{q}}) + \boldsymbol{g}(\boldsymbol{q}) \Longleftrightarrow \boldsymbol{Q} = \boldsymbol{A}(\boldsymbol{q}, \dot{\boldsymbol{q}}, \ddot{\boldsymbol{q}})\boldsymbol{p}. \tag{6}$$

The left-hand side of Eq. (6) shows the conventional form of the dynamic equations, whereas on the right side, the parameter-linear form of the equation of motion is given. The mass matrix $\boldsymbol{M}(\boldsymbol{q})$ is a function of the joint angles $\boldsymbol{q}$; $\boldsymbol{c}(\boldsymbol{q}, \dot{\boldsymbol{q}})$ describes centrifugal and Coriolis effects and $\boldsymbol{g}(\boldsymbol{q})$ resembles the influence of gravitation. $\boldsymbol{Q}$ is the vector of joint torques. The matrix $\boldsymbol{A}(\boldsymbol{q}, \dot{\boldsymbol{q}}, \ddot{\boldsymbol{q}})$ contains the known kinematic quantities of the robot, which is multiplied by the corresponding parameter vector $\boldsymbol{p}$.

The moments of inertia of the motors I_{mi} are usually given by the manufacturer so that they are not included in the identification model. Nevertheless, they have to be compensated by means of an additional model

$$\boldsymbol{Q}_m = \boldsymbol{H}(\boldsymbol{q})\ddot{\boldsymbol{q}} + \boldsymbol{c}_m(\boldsymbol{q}, \dot{\boldsymbol{q}}) \tag{7}$$

as described in Daemi and Heimann (1998).

4.3. Determination of base parameters

For application of LS-estimation techniques (Lawson and Hanson, 1974), the parameter vector $\boldsymbol{p}$ must have minimal dimension (referred to as *base parameter vector*). This means that all parameters without influence must be removed at first. For example, a revolute base axis can be regarded. If the base is fixed, obviously only one element (I_{zz1}) in $\boldsymbol{I}_1^{(1)}$ has an influence on the dynamics. Second, the parameters must be regrouped in order to eliminate all linear dependencies from $\boldsymbol{A}(\boldsymbol{q},\dot{\boldsymbol{q}},\ddot{\boldsymbol{q}})$ so that it becomes a full rank matrix.

The determination of the base parameter vector is demanding, especially for robots with more than three degrees of freedom (d.o.f.). One possibility is the use of numerical methods, like *singular-value-decomposition* (Gautier, 1990; Pfeiffer and Hölzl, 1995). The main disadvantage of this approach is that the determination of the new parameter combinations is difficult and very time consuming.

Gautier and Khalil presented an analytical method in 1988. Their algorithm is based on a recursive *Lagrange* algorithm. General rules were formulated for calculating the energy contributions of the parameters of link i with respect to those of link $i-1$. These rules were further exploited to find a recursive algorithm to calculate the base parameters.

4.4. Grouping of the base parameters and the dynamic equations

The two-step identification scheme presented in Section 6 is based on partitioning the base parameters into three vectors:

1. The gravitational parameters $\boldsymbol{p}_{\mathrm{g}}$ occur in $\boldsymbol{g}(\boldsymbol{q})$.
2. The diagonal parameters $\boldsymbol{p}_{\mathrm{Md}}$ occur on the diagonal of $\boldsymbol{M}(\boldsymbol{q})$ but not in $\boldsymbol{g}(\boldsymbol{q})$.
3. The off-diagonal parameters $\boldsymbol{p}_{\mathrm{Mod}}$ occur only in the off-diagonal elements of $\boldsymbol{M}(\boldsymbol{q})$.

The grouping property holds for any open kinematic chain, i.e. for typical serial industrial robots. Furthermore, typically the number of elements of $\boldsymbol{p}_{\mathrm{Mod}}$ is small due the symmetric structure of the links, e.g. for the *manutec-r15*, $\boldsymbol{p}_{\mathrm{Mod}}$ has only one element. The grouping leads to a separation of matrix $\boldsymbol{A}(\boldsymbol{q},\dot{\boldsymbol{q}},\ddot{\boldsymbol{q}})$ in Eq. (6) into different components:

$$\boldsymbol{Q} = \underbrace{\boldsymbol{A}_{\mathrm{Md}}(\boldsymbol{q},\ddot{\boldsymbol{q}})\boldsymbol{p}_{\mathrm{Md}} + \boldsymbol{A}_{\mathrm{Mod}}(\boldsymbol{q},\ddot{\boldsymbol{q}})\boldsymbol{p}_{\mathrm{Mod}} + \boldsymbol{A}_{\mathrm{Mg}}(\boldsymbol{q},\ddot{\boldsymbol{q}})\boldsymbol{p}_{\mathrm{g}}}_{\boldsymbol{M}(\boldsymbol{q})\ddot{\boldsymbol{q}}} + \underbrace{\boldsymbol{A}_{\mathrm{c}}(\boldsymbol{q},\dot{\boldsymbol{q}})\boldsymbol{p}}_{\boldsymbol{c}(\boldsymbol{q},\dot{\boldsymbol{q}})} + \underbrace{\boldsymbol{A}_{\mathrm{g}}(\boldsymbol{q})\boldsymbol{p}_{\mathrm{g}}}_{\boldsymbol{g}(\boldsymbol{q})}. \tag{8}$$

Of course, the parameter vectors are still coupled by $\boldsymbol{c}(\boldsymbol{q},\dot{\boldsymbol{q}})$. Nevertheless, they can be separately identified since this coupling is eliminated by a proper choice of identification measurements (Section 6.3).

5. Conventional identification scheme

There exists a vast amount of literature on the identification of the rigid body model (Armstrong, 1988, 1989; Daemi and Heimann, 1996; Daemi and Grotjahn, 1996; Gautier and Khalil, 1988b; Gautier et al., 1995; Pfeiffer and Hölzl, 1995; Khosla, 1988; Khosla and Kanade, 1987; Presse and Gautier, 1993; Prüfer et al., 1994). However, most of the methods are variations of the same identification scheme. The robot is moved along a trajectory, where joint motion and torque are measured. Finally, the parameters are estimated by the use of the LS technique.

5.1. Least-squares estimation

The LS identification is based on the representation of robot dynamics shown on the right-hand side of Eq. (6). For a certain point in time t_k, measurements of $m \leqslant n$ different axes $\gamma_1, \ldots, \gamma_m$ are combined as

$$\boldsymbol{Q}_{t_k} = \left[Q_{\gamma_1,t_k} \ \ldots \ Q_{\gamma_m,t_k}\right]^{\mathrm{T}} \quad \text{and} \quad \boldsymbol{\Psi}_{t_k} = \left[\boldsymbol{A}^{\mathrm{T}}_{\gamma_1,t_k} \ \ldots \ \boldsymbol{A}^{\mathrm{T}}_{\gamma_m,t_k}\right]^{\mathrm{T}} \tag{9}$$

with Q_{γ_j,t_k}, the torque of joint γ_j and $\boldsymbol{A}_{\gamma_j,t_k}$, the corresponding row of $\boldsymbol{A}(\boldsymbol{q}(t_k), \dot{\boldsymbol{q}}(t_k), \ddot{\boldsymbol{q}}(t_k))$. Further combination of measurements at r ($r \cdot m \gg n$) different time steps leads to the over-determined vector equation,

$$\boldsymbol{Q} = \boldsymbol{\Psi}\boldsymbol{p} + \boldsymbol{e}, \tag{10}$$

with the measurement vector $\boldsymbol{Q} = \left[\boldsymbol{Q}_{t_1} \ldots \boldsymbol{Q}_{t_r}\right]^{\mathrm{T}}$, the observation matrix $\boldsymbol{\Psi} = \left[\boldsymbol{\Psi}^{\mathrm{T}}_{t_1} \ldots \boldsymbol{\Psi}^{\mathrm{T}}_{t_r}\right]^{\mathrm{T}}$ and the unknown error $\boldsymbol{e}$ which has to be introduced due to measurement noise. The general solution for Eq. (10) can be found by a pseudo-inverse of the observation matrix:

$$\hat{\boldsymbol{p}} = (\widetilde{\boldsymbol{\Psi}}^{\mathrm{T}}\boldsymbol{\Psi})^{-1}\widetilde{\boldsymbol{\Psi}}^{\mathrm{T}}\boldsymbol{Q}. \tag{11}$$

This shows why $\boldsymbol{p}$ has to have minimal dimension. Otherwise, $\boldsymbol{\Psi}$ would not have full rank and the pseudo-inverse would not exist. The most common definition of $\widetilde{\boldsymbol{\Psi}}$ is $\widetilde{\boldsymbol{\Psi}} = \boldsymbol{\Psi}$ which leads to a minimum of the error vector $\boldsymbol{e}$ in the LS sense:

$$\hat{\boldsymbol{p}}_{\mathrm{LS}} = \min_{\boldsymbol{p}}\left(\boldsymbol{e}^{\mathrm{T}}\boldsymbol{e}\right) \Rightarrow \hat{\boldsymbol{p}}_{\mathrm{LS}} = \left(\boldsymbol{\Psi}^{\mathrm{T}}\boldsymbol{\Psi}\right)^{-1}\boldsymbol{\Psi}^{\mathrm{T}}\boldsymbol{Q}. \tag{12}$$

Relation (12) is the most general case that does not take into account any a priori information of the system or disturbances. In the literature, a lot of refinements can be found. Seeger (1992) proposed weighting with maximal joint torque to account for the different torque ranges of the drives. Gautier and Khalil (1992) suggested another weighting method using expected values of the parameters. Other well-known refinements are the *instrumental variable* method (Seeger, 1992) or the *total least-squares* estimation (Gautier et al., 1994).

5.2. Trajectory optimisation

A sufficient excitation of all parameters is necessary to ensure their identifiability. If one or more parameters are not excited, $\boldsymbol{\Psi}$ loses its full rank and Eq. (11) cannot be solved. However, already a poor excitation leads to a large influence of disturbances on the estimation result. An upper bound for the relative error of the estimated parameter vector is given by (Armstrong, 1988; Lawson and Hanson, 1974)

$$\frac{\left\|\boldsymbol{p} - \hat{\boldsymbol{p}}\right\|}{\|\boldsymbol{p}\|} \leqslant \mathrm{cond}(\boldsymbol{\Psi})\frac{\|\boldsymbol{e}\|}{\|\boldsymbol{Q}\|} \quad \text{with} \quad \mathrm{cond}(\boldsymbol{\Psi}) = \frac{\sigma_{\max}(\boldsymbol{\Psi})}{\sigma_{\min}(\boldsymbol{\Psi})} \tag{13}$$

and $\sigma_{\max}(\boldsymbol{\Psi})$ and $\sigma_{\min}(\boldsymbol{\Psi})$ is the largest and smallest singular value of $\boldsymbol{\Psi}$, respectively. By minimising the condition of the observation matrix, the standard criterion for trajectory optimisation is defined (Armstrong 1988, 1989; Gautier and Khalil, 1988b; Pfeiffer and Hölzl, 1995). Other optimisation criteria, like maximisation of the smallest singular value, can be found in Armstrong (1988, 1989), Presse and Gautier (1993), Shaefers et al. (1993) and Daemi and Grotjahn (1996).

One disadvantage of the optimisation is the computational burden (Armstrong, 1988, 1989; Daemi and Grotjahn, 1996; Gautier and Khalil, 1992). The main problem, however, is that the robot control must provide the possibility of driving arbitrary trajectories. With standard industrial controls, however, only very simple trajectories (line, circles, ptp) can be generated.

5.3. Friction compensation

The most common way of compensating the influence of friction on rigid body identification is to perform 'warm-up' motions to reach stationary temperature and lubrication conditions. Then, the rigid body model is identified together with the friction model (Gautier and Khalil, 1988b; Prüfer et al., 1994; Pfeiffer and Hölzl, 1995). The disadvantage of this approach is the large number of parameters which results from the more complex friction models (2) and (3). For example, for a six d.o.f. robot, it would lead to 18 additional parameters which would make the identification much more complex or even impossible.

The other possibility is to compensate friction by a model identified in advance (Daemi and Heimann, 1996). As shown in Section 3, however, the operating conditions change so fast that an exact friction compensation is impossible. This leads to systematic errors in rigid body identification.

6. Two-step identification

In Section 5, the conventional identification scheme and its main disadvantages – the need of optimised trajectories and model-based friction compensation – are discussed. In this section, a different approach is introduced which eliminates these disadvantages.

6.1. Identification scheme

The identification scheme is based on the grouping of the base parameters presented in Section 4.4. In the first step, the elements of $\boldsymbol{g}(\boldsymbol{q})$ and $\boldsymbol{M}(\boldsymbol{q})$ are 'measured' for a number of different joint configurations (Sections 6.2 and 6.3). In the second step, parameters are estimated by a combined evaluation of the separate measurements.

The measuring of the gravitational torque at m different joint configurations and the combination of all these measurements leads to

$$\underbrace{\begin{bmatrix} Q_{\gamma_1}^{(1)} \\ \vdots \\ Q_{\gamma_m}^{(m)} \end{bmatrix}}_{\boldsymbol{\Gamma}_\mathrm{g}} = \underbrace{\begin{bmatrix} \boldsymbol{A}_{\mathrm{g},\gamma_1}\left(\boldsymbol{q}^{(1)}\right) \\ \vdots \\ \boldsymbol{A}_{\mathrm{g},\gamma_m}\left(\boldsymbol{q}^{(m)}\right) \end{bmatrix}}_{\boldsymbol{\Psi}_\mathrm{g}} \boldsymbol{p}_\mathrm{g} + \underbrace{\begin{bmatrix} e^{(1)} \\ \vdots \\ e^{(m)} \end{bmatrix}}_{\boldsymbol{e}_\mathrm{g}}, \tag{14}$$

where $Q_{\gamma_i}^{(n)}$ are the measured gravitational torques, $\boldsymbol{A}_{\mathrm{g},\gamma_i}\left(\boldsymbol{q}^{(i)}\right)$ are the corresponding rows of $\boldsymbol{A}_\mathrm{g}(\boldsymbol{q})$ for the given joint configuration, $\boldsymbol{q}^{(i)}$ and $\boldsymbol{e}^{(i)}$ are the unknown measurement errors. Suitable joint configurations are selected by analysis of the gravitational vector $\boldsymbol{g}(\boldsymbol{q})$ (Section 6.2). The application of a weighted LS estimation leads to

$$\hat{\boldsymbol{p}}_\mathrm{g} = \min_{\boldsymbol{p}_\mathrm{g}}\left(\boldsymbol{e}_\mathrm{g}^\mathrm{T}\boldsymbol{W}\boldsymbol{e}_\mathrm{g}\right) \Rightarrow \hat{\boldsymbol{p}}_\mathrm{g} = \left(\boldsymbol{\Psi}_\mathrm{g}^\mathrm{T}\boldsymbol{W}\boldsymbol{\Psi}_\mathrm{g}\right)^{-1}\boldsymbol{\Psi}_\mathrm{g}^\mathrm{T}\boldsymbol{W}\boldsymbol{\Psi}_\mathrm{g}. \tag{15}$$

The diagonal weighting matrix takes into account the different ranges of the torque measurements by weighting them with the maximum torque of each axis

$$\boldsymbol{W} = \mathrm{diag}\left(w_{\gamma_1} \ldots w_{\gamma_m}\right) \quad \text{with} \quad w_{\gamma_i} = Q_{\gamma_i,\max}^{-1}. \tag{16}$$

Next, $\boldsymbol{p}_\mathrm{Md}$ is identified by measuring diagonal elements of the mass matrix M_{ii} (see $\hat{M}_{ii}$ in Section 6.3) at k different operating points which are chosen by analysing $\boldsymbol{M}(\boldsymbol{q})$ (Section 6.2). These measurements are

combined and the influence of the already known $\hat{\boldsymbol{p}}_{\mathrm{g}}$ is compensated as well as the diagonal elements H_{ii} of the mass matrix $\boldsymbol{H}(\boldsymbol{q})$

$$\underbrace{\begin{bmatrix} \hat{M}^{(1)}_{\gamma_1} \\ \vdots \\ \hat{M}^{(k)}_{\gamma_k} \end{bmatrix} - \begin{bmatrix} \boldsymbol{A}_{\mathrm{Mg},\gamma_1}\left(\boldsymbol{q}^{(1)}, \boldsymbol{u}_{\gamma_1}\right) \\ \vdots \\ \boldsymbol{A}_{\mathrm{Mg},\gamma_k}\left(\boldsymbol{q}^{(k)}, \boldsymbol{u}_{\gamma_k}\right) \end{bmatrix} \hat{\boldsymbol{p}}_{\mathrm{g}} - \begin{bmatrix} H^{(1)}_{\gamma_1} \\ \vdots \\ H^{(k)}_{\gamma_k} \end{bmatrix}}_{\boldsymbol{\Gamma}_{\mathrm{Md}}} = \underbrace{\begin{bmatrix} \boldsymbol{A}_{\mathrm{Md},\gamma_1}\left(\boldsymbol{q}^{(1)}, \boldsymbol{u}_{\gamma_1}\right) \\ \vdots \\ \boldsymbol{A}_{\mathrm{Md},\gamma_k}\left(\boldsymbol{q}^{(k)}, \boldsymbol{u}_{\gamma_k}\right) \end{bmatrix}}_{\boldsymbol{\Psi}_{\mathrm{Md}}} \boldsymbol{p}_{\mathrm{Md}} + \underbrace{\begin{bmatrix} e^{(1)} \\ \vdots \\ e^{(k)} \end{bmatrix}}_{\boldsymbol{e}_{\mathrm{Md}}}. \tag{17}$$

The compensation of $\hat{\boldsymbol{p}}_{\mathrm{g}}$ does not significantly worsen the estimation result. The measurements of the elements of $\boldsymbol{g}(\boldsymbol{q})$ are very simple and a relatively high precision of $\hat{\boldsymbol{p}}_{\mathrm{g}}$ can be achieved. The vector $\boldsymbol{u}_{\gamma_i}$ is a vector of same size as $\dot{\boldsymbol{q}}$ with a 1 in the component γ_i of the measured inertia and zeroes elsewhere. This means that Eq. (17) has the dimension of a moment of inertia for rotational joints and the dimension of a mass for translational joints. An estimation for $\boldsymbol{p}_{\mathrm{Md}}$ can then be found by

$$\hat{\boldsymbol{p}}_{\mathrm{Md}} = \min_{\boldsymbol{p}_{\mathrm{Md}}}\left(\boldsymbol{e}^{\mathrm{T}}_{\mathrm{Md}}\boldsymbol{W}\boldsymbol{e}_{\mathrm{Md}}\right) \Rightarrow \hat{\boldsymbol{p}}_{\mathrm{Md}} = \left(\boldsymbol{\Psi}^{\mathrm{T}}_{\mathrm{Md}}\boldsymbol{W}\boldsymbol{\Psi}_{\mathrm{Md}}\right)^{-1}\boldsymbol{\Psi}^{\mathrm{T}}_{\mathrm{Md}}\boldsymbol{W}\boldsymbol{\Psi}_{\mathrm{Md}}. \tag{18}$$

The identification of $\boldsymbol{p}_{\mathrm{Mod}}$ is completely analogous to Eqs. (17) and (18). The difference lies in the execution of the measurement, where acceleration of one axis is related to the torque of another axis (Daemi and Heimann, 1998). Finally, $\hat{\boldsymbol{p}}_{\mathrm{g}}$, $\hat{\boldsymbol{p}}_{\mathrm{Md}}$ and $\hat{\boldsymbol{p}}_{\mathrm{Mod}}$ are combined to $\hat{\boldsymbol{p}}$.

6.2. Choice of joint configurations

It must be ensured that all parameters are sufficiently excited. The influence of one special parameter in $\boldsymbol{g}(\boldsymbol{q})$ and $\boldsymbol{M}(\boldsymbol{q})$ depends on the joint angles. This dependence is excited by varying the joint configuration. As an example, one can regard the fourth diagonal element of $\boldsymbol{M}(\boldsymbol{q})$ of the *manutec-r15*: $M_{44} = p_{10} + p_{11}\sin^2(q_5) + p_{14}\cos^2(q_5)$. The parameters p_{10}, p_{11} and p_{14} can be excited and estimated by varying q_5 for different measurements of M_{44}. In our experiment, for example, we changed q_5 from $-100°$ to $100°$ in steps of 25°. An analogous analysis and variation of all angular dependencies in $\boldsymbol{g}(\boldsymbol{q})$ and $\boldsymbol{M}(\boldsymbol{q})$ yields relatively good results for the characteristic values of the estimation problem, like condition number or smallest singular value. Therefore, an optimisation is not necessary to ensure sufficient excitation.

6.3. Measurement trajectories

A major advantage of the measurements at operating points is the fact that they can be implemented easily in typical industrial robot controls. Each measurement is carried out by moving the axis 'back and forth' along some trapezoidal velocity profile in the neighbourhood of the operating point. No optimisation strategy is necessary as only one quantity is interesting and the trajectories have a special characteristic to ensure excitation of this quantity.

For measurements of gravitational torques, long periods with constant velocity have to be included (Fig. 3a) in order to excite gravitational effects and to eliminate inertial influences. The mean value between an averaged torque at forward and backward motion gives the desired gravitational torque.

Motions with a higher share of acceleration are used to identify the moments of inertia (Fig. 3b). The gravitational component is compensated and a joint model

$$Q_i = M_{ii}\ddot{q}_i + a_1\dot{q}_i + a_2\mathrm{sign}(\dot{q}_i) + a_3\dot{q}_i^{1/3} \tag{19}$$

is adapted to the measurement again by use of a LS estimation

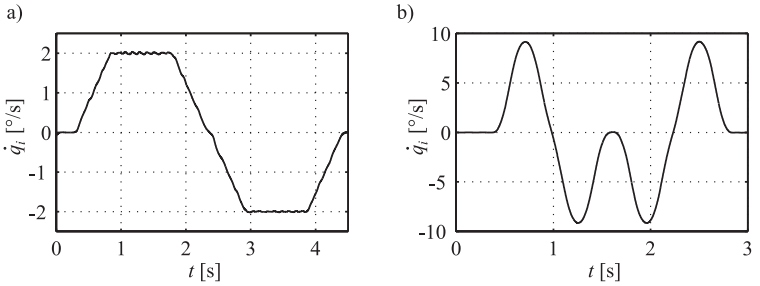

Fig. 3. Typical trajectories for identification of (a) gravitational and (b) inertial parameters.

$$\boldsymbol{\Psi} = \begin{bmatrix} \ddot{q}_i(t_1) & \dot{q}_i(t_1) & \operatorname{sign}\left(\dot{q}_i(t_1)\right) & \dot{q}_i^{1/3}(t_1) \\ \vdots & \vdots & \vdots & \vdots \\ \ddot{q}_i(t_r) & \dot{q}_i(t_r) & \operatorname{sign}\left(\dot{q}_i(t_r)\right) & \dot{q}_i^{1/3}(t_r) \end{bmatrix}, \qquad \boldsymbol{\Gamma} = \begin{bmatrix} Q_i(t_1) \\ \vdots \\ Q_i(t_r) \end{bmatrix} \Rightarrow \hat{\boldsymbol{p}}_{\mathrm{r}} = \left(\boldsymbol{\Psi}^{\mathrm{T}}\boldsymbol{\Psi}\right)^{-1}\boldsymbol{\Psi}^{\mathrm{T}}\boldsymbol{\Gamma} \tag{20}$$

with $\hat{\boldsymbol{p}}_{\mathrm{r}} = \left[\hat{M}_{ii}, \hat{a}_1, \hat{a}_2, \hat{a}_3\right]^{\mathrm{T}}$.

The measurement of the off-diagonal elements of the inertia matrix is similar to the gravitational measurements. Axis i is moved at a very low constant velocity to avoid sticking and axis j is accelerated in the neighbourhood of the operating point. Since speed of axis i is constant, a very simple linear friction model is applied

$$Q_j = M_{ji}\ddot{q}_i + a_1\dot{q}_j. \tag{21}$$

Finally, the coupling inertia M_{ji} is identified similarly to Eq. (20).

The coupling expressed by $\boldsymbol{c}(\boldsymbol{q}, \dot{\boldsymbol{q}})$ (Section 4.4) has no influence on the measurements of gravitational torques and the diagonal elements of the mass matrix. The element of $\boldsymbol{c}(\boldsymbol{q}, \dot{\boldsymbol{q}})$ that corresponds to the measured torque becomes zero since only this single axis is moved. For the measurements of the off-diagonal elements of the mass matrix, however, the influence of $\boldsymbol{c}(\boldsymbol{q}, \dot{\boldsymbol{q}})$ is not zero in general. But it can usually be neglected as both axes are moved at low velocity.

7. Experimental set-up

The test stand consists of the commercial robot *Siemens manutec-r15* and its standard control *ACR-20*. The measurements are carried out by a *dSPACE* real-time computer which is connected to a *WinNT-PC* with the program package MATLAB/SIMULINK.

7.1. Measurement and signal processing

For the identification joint positions and driving torques are obtained from the motor encoder signals and motor currents. Velocities and accelerations are calculated by numerical differentiation. All measurements are filtered with a non-causal, phase-neutral eighth-order *Butterworth* low-pass filter. Although all signals are measured on the motor side, the influence of gear elasticity and backlash can be neglected since only shock- and jerk-less trajectories are used.

7.2. The industrial robot Siemens manutec-r15

The *Siemens manutec-r15* is a six d.o.f. industrial robot with revolute joints. In Fig. 4, the definition of the MDH coordinate frames and parameters are given. As mentioned in Section 4.1, a lot of parameters can be set to zero since they have no influence on the dynamics. Table 1 shows the remaining elements of the $\boldsymbol{p}_{\mathrm{link},i}$ for all links. The application of Gautier and Khalil's algorithm (1988) to these definitions leads to the base parameter vector

$$\boldsymbol{p} = \begin{bmatrix} p_1 \\ p_2 \\ p_3 \\ p_4 \\ p_5 \\ p_6 \\ p_7 \\ p_8 \\ p_9 \\ p_{10} \\ p_{11} \\ p_{12} \\ p_{13} \\ p_{14} \end{bmatrix} = \begin{bmatrix} I_{zz1} + I_{yy2} + I_{yy3} + l_1^2(m_3 + m_4 + m_5 + m_6) \\ I_{xx2} - I_{yy2} - l_1^2(m_3 + m_4 + m_5 + m_6) \\ I_{xz2} \\ I_{zz2} + l_1^2(m_3 + m_4 + m_5 + m_6) \\ s_{x2} + l_1(m_3 + m_4 + m_5 + m_6) \\ I_{xx3} - I_{yy3} + I_{yy4} + 2l_2 s_{z4} + l_2^2(m_4 + m_5 + m_6) \\ I_{zz3} + I_{yy4} + 2l_2 s_{z4} + l_2^2(m_4 + m_5 + m_6) \\ s_{y3} - s_{z4} - l_2(m_4 + m_5 + m_6) \\ I_{xx4} + I_{yy5} - I_{yy4} \\ I_{zz4} + I_{yy5} \\ I_{xx5} + I_{xx6} - I_{yy5} \\ I_{zz5} + I_{xx6} \\ s_{y5} - s_{z6} \\ I_{zz6} \end{bmatrix}. \tag{22}$$

The influence of the base parameters on $\boldsymbol{g}(\boldsymbol{q})$ and $\boldsymbol{M}(\boldsymbol{q})$ are given in Table 2. It shows that the base parameters can be divided according to Eq. (8) into three groups:

1. p_5, p_8, p_{13} are the only parameters contained in $\boldsymbol{g}(\boldsymbol{q})$. They are combined in $\boldsymbol{p}_{\mathrm{g}}$.
2. All remaining parameters with the exception of p_3 can be found on the diagonal elements of $\boldsymbol{M}(\boldsymbol{q})$. They are combined in $\boldsymbol{p}_{\mathrm{Md}}$.

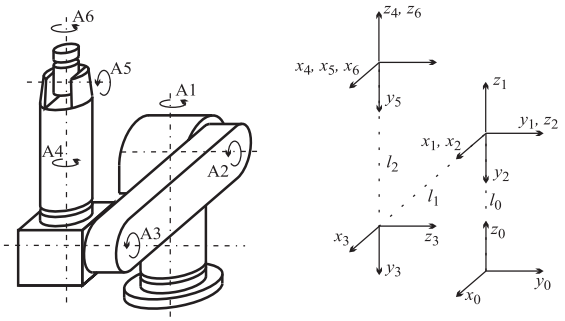

i	θ_i	d_i	α_i	a_i
1	$-q_1$	l_0	0	0
2	q_2	0	0	$-\pi/2$
3	$q_3+\pi/2$	0	l_1	0
4	$-q_4$	l_2	0	$\pi/2$
5	q_5	0	0	$-\pi/2$
6	q_6	0	0	$\pi/2$

Fig. 4. MDH coordinate frames and parameters for the *manutec-r15*.

Table 1
Non-negligible parameters of the *manutec-r15*

$\boldsymbol{p}_{\mathrm{link},1}$	$\boldsymbol{p}_{\mathrm{link},2}$	$\boldsymbol{p}_{\mathrm{link},3}$	$\boldsymbol{p}_{\mathrm{link},4}$	$\boldsymbol{p}_{\mathrm{link},5}$	$\boldsymbol{p}_{\mathrm{link},6}$
I_{zz1}	$I_{xx2}, I_{xz2}, I_{yy2}, I_{zz2}, s_{x2}$	$I_{xx3}, I_{yy3}, I_{zz3}, s_{y3}, m_3$	$I_{xx4}, I_{yy4}, I_{zz4}, s_{z4}, m_4$	$I_{xx5}, I_{yy5}, I_{zz5}, s_{y5}, m_5$	$I_{xx6}, I_{yy6}, I_{zz6}, s_{z6}, m_6$

Table 2
Dependencies of $\boldsymbol{g}(\boldsymbol{q})$ and $\boldsymbol{M}(\boldsymbol{q})$ on $\boldsymbol{p}$ for the *manutec-r15*

$M_{ij}(\boldsymbol{q})$	$j=1$	$j=2$	$j=3$	$j=4$	$j=5$	$j=6$	$g_i(\boldsymbol{q})$
$i=1$	$p_1,p_2,p_6,p_8,p_9,p_{10},$ $p_{11},p_{12},p_{13},p_{14}$	$p_3,p_9,p_{11},p_{12},p_{13},p_{14}$	$p_9,p_{11},p_{12},p_{13},p_{14}$	$p_{10},p_{11},p_{13},p_{14}$	p_{12},p_{13}	p_{14}	0
$i=2$	Sym.	$p_4,p_7,p_8,p_9,p_{11},$ p_{12},p_{13},p_{14}	$p_7,p_8,p_9,p_{11},p_{12},$ p_{13},p_{14}	p_{11},p_{13},p_{14}	p_{12},p_{13}	p_{14}	p_5,p_8,p_{13}
$i=3$	Sym.	Sym.	$p_7,p_9,p_{11},p_{12},p_{13},p_{14}$	p_{11},p_{13},p_{14}	p_{12},p_{13}	p_{14}	p_8,p_{13}
$i=4$	Sym.	Sym.	Sym.	p_{10},p_{11},p_{14}	0	p_{14}	p_{13}
$i=5$	Sym.	Sym.	Sym.	Sym.	p_{12}	0	p_{13}
$i=6$	Sym.	Sym.	Sym.	Sym.	Sym.	p_{14}	0

3. For this robot p_3 is the only parameter that can only be found on the off-diagonal elements of $\boldsymbol{M}(\boldsymbol{q})$ and thus, has to be identified by measuring coupling torque.

A more complete description of the robot is given in Daemi and Heimann (1998) and Daemi (1998).

8. Results

The algorithm described in this paper is applied to the *manutec-r15*. For the identification of $\boldsymbol{p}_{\mathrm{g}}$, measurements at 64 joint configurations are used, 92 configurations for $\boldsymbol{p}_{\mathrm{Md}}$ and nine configurations for $\boldsymbol{p}_{\mathrm{Mod}}$. The duration for all measurements is about 45 min. A second series of measurements is carried out with an additional load of 10.86 kg mounted on the end effector. The distance of its centre of mass to the hand wrist is 140 mm. Figs. 5 and 6 give a comparison of the measured gravitational torques and moments of inertia with those modelled by the identified parameter vectors. The dependencies on the joint angles are accurately

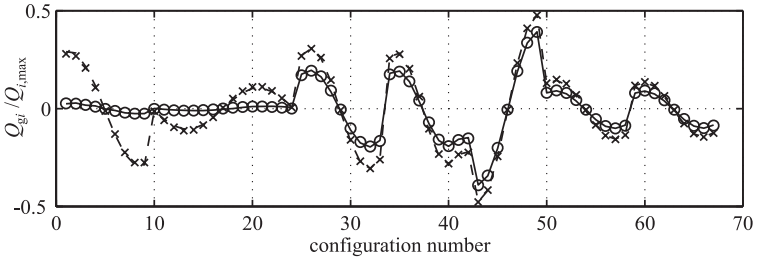

Fig. 5. Gravitational torques with (×) and without (○) additional mass compared to their model representation (— and - - -).

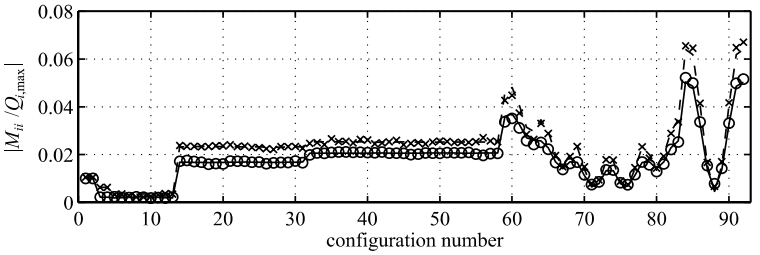

Fig. 6. Moments of inertia with (×) and without (○) additional mass compared to their model representation (— and - - -).

Table 3
Identification results for *manutec-r15* with (A) and without additional (B) payload

i	1	2	3	4	5	6	7
p_i(A)	32.015	−28.058	−2.187	19.905	48.491	9.602	13.313
p_i(B)	36.907	−33.782	−2.435	22.565	51.896	16.331	18.562
Δp_i	4.892	−5.724	−0.247	2.6597	3.405	6.7296	5.2493
Δp_i(exp.)	2.713	−2.713	0	2.713	5.409	5.786	5.786
i	8	9	10	11	12	13	14
p_i(A)	−15.836	0.0000	0.0443	0.2883	0.1554	−0.1885	0.3760
p_i(B)	−23.244	−0.0895	0.2198	0.2274	0.4381	−1.9983	0.3980
Δp_i	−7.408	−0.0895	0.1755	−0.0609	0.2826	−1.8097	0.0220
Δp_i(exp.)	−7.885	0.0	0.0	0.0	0.0	−1.518	0.0470

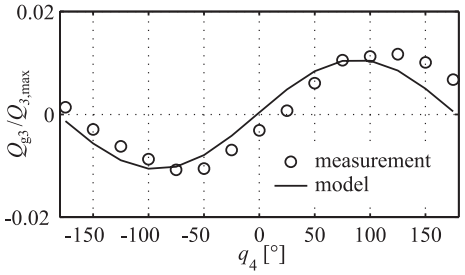

Fig. 7. Clipping from Fig. 6 without additional mass (configuration number 10–24).

reflected by the model and the influence of the additional mass is obvious. Many of the measured moments of inertia are constant with respect to changing joint configuration. But the main reason for this behaviour is the chosen representation in which the influence of the gravitational parameters is compensated. They contribute significantly to the angular dependency since they reflect contributions due to *Steiner's* theorem.

Numerical results for the base parameters with and without additional mass are shown in Table 3. The differences between the two identification results are also given, which reflect the influence of the additional mass. They are compared to their expected values resulting from the base parameter definition in Eq. (22). It has to be considered that due to the compensation of the motor inertia and the friction, only a small fraction of the measured torques contain information for the identification process. Especially, for parameters with higher indices results become more inaccurate because the influence of friction in the hand axes increases. Still, the increase of parameters is well reflected in the measurements indicating a successful identification of the complex dynamics of the robotic system.

Besides simplicity of the measurements and no need of model-based friction compensation, another advantage of this method becomes visible. By analysing the measurements, an evaluation of the model structure is possible to find unmodelled effects as well as unnecessary parameters. An example is given in Fig. 7, where the gravitational torque of joint 3 is plotted as a function joint angle four. An offset of about 30° of the measured sinusoidal torque characteristic is observable which cannot be reflected by the model. This is due to the unmodelled distance of the centre of mass of joint four to its rotational axis.

9. Conclusions

The conventional model consisting of dry friction and viscous damping is usually not sufficient for the modelling of friction losses in industrial robots' gears. But even by more complex models, the change of

friction with respect to temperature and lubrication conditions cannot be reflected with maintainable effort. The lack of predictability can lead to a deterioration of rigid body identification. The presented identification method eliminates this disadvantage. Furthermore, it is much easier to apply to standard industrial robots since only simple trajectories with trapezoidal velocity profile are used. The third main advantage of the presented method is the possibility of evaluating the model by investigation of the measurements. The efficiency of the method is illustrated by experimental application to the standard industrial robot *manutec-r15*.

References

Armstrong, B., 1988. Dynamics for robot control: Friction modeling and ensuring excitation during parameter identification. Stanford University, Stanford, CA, 1988.

Armstrong, B., 1989. On finding exiting trajectories for identification experiments involving systems with nonlinear dynamics. Int. J. Robotics Res. 8 (6), 28–48.

Armstrong-Hélouvry, B., 1991. Control of Machines with Friction. Kluwer Academic Publishers, Boston.

Armstrong-Hélouvry, B., Dupont, P., Canudas de Wit, C., 1994. A survey of models, analysis tools and compensation methods for the control of machines with friction. Automatica 30 (7), 1083–1138.

Canudas de Wit, C., Noel, P., Aubin, A., Brogliato, B., 1991. Adaptive friction compensation in robot manipulators: low velocities. The Int. J. Robotics Res. 10 (3), 189–199.

Daemi, M., 1998. Modellierung und Identifikation der Dynamik von Industrierobotern für den Einsatz in Regelungen. Fortschritt-Berichte VDI. VDI-Verlag, Düsseldorf (in German).

Daemi, M., Grotjahn, M., 1996. Practical experiences with L.S. methods for the identification of robot dynamics. In: Proc. of the 2nd ECPD International Conference on Advanced Robotics, Vienna.

Daemi, M., Heimann, B., 1996. Identification and compensation of gear friction for modeling of robots. In: Proc. of the 11th CISM-IFToMM Symp. on the Theory and Practice of Robots and Manipulators, Udine, pp. 89–96.

Daemi, M., Heimann, B., 1998. Separation of friction and rigid body identification for industrial robots. In: Proc. of the 11th CISM-IFToMM Symp. on the Theory and Practice of Robots and Manipulators, Paris, pp. 35–42.

Gautier, M., 1990. Numerical calculation of the base inertial parameters. In: Proc. of the IEEE Int. Conf. on Robotics and Automation, Cincinati, pp. 1020–1025.

Gautier, M., Khalil, W., 1988a. A direct determination of minimum inertial parameters of robots. In: Proc. of the IEEE Int. Conf. on Robotics and Automation, pp. 1682–1687.

Gautier, M., Khalil, W., 1988b. On the identification of the inertial parameters of robots. In: Proc. of the IEEE Conf. on Decision and Control, pp. 2264–2269.

Gautier, M., Khalil, W., 1992. Exciting trajectories for the identification of base inertial parameters of robots. Int. J. Robotics Res. 11, 362–375.

Gautier, M., Khalil, W., Restrepo, P.P., 1995. Identification of the dynamic parameters of a closed loop robot. In: Proc. of the IEEE Int. Conf. on Robotics and Automation, Nagoya, pp. 3045–3050.

Gautier, M., Vandanjon, P.O., Presse, C., 1994. Identification of inertial and drive gain parameters of robots. In: Proc. of the IEEE Conf. on Decision and Control, Lake Buena Vista, pp. 3764–3769.

Khalil, W., Kleinfinger, J.F, 1986. A new geometric notation for open and closed-loop robots. In: Proc. of the IEEE Int. Conf. on Robotics and Automation, pp. 1174–1179.

Khosla, P.K., 1988. Estimation of robot dynamics parameters: theory and application. Int. J. Robotics and Automation 3 (1), 35–40.

Khosla, P.K., Kanade, T., 1987. An algorithm to estimate manipulator dynamics parameters. Int. J. Robotics and Automation 2 (3), 127–135.

Lawson, C.L., Hanson, R.J., 1974. Solving Least Squares Problems. Prentice-Hall, Englewood Cliffs, NJ.

Pfeiffer, F., Hölzl, J., 1995. Parameter identification for industrial robots. In: Proc. of the IEEE Int. Conf. on Robotics and Automation, Nagoya, pp. 1468–1476.

Presse, C., Gautier, M., 1993. New criteria of exciting trajectories for robot identification. In: Proc. of the IEEE Int. Conf. on Robotics and Automation, Atlanta, pp. 907–912.

Prüfer, M., Schmidt, C., Wahl, F., 1994. Identification of robot dynamics with differential and integral models: a comparison. In: Proc. of the IEEE Int. Conf. on Robotics and Automation, San Diego, pp. 340–345.

Prüfer, M., Wahl, F., 1994. Friction analysis and modelling for geared robots. In: Proc. of the 4th IFAC Symposium on Robot Control, Capri, pp. 551–556.

Seeger, G., 1992. Selbsteinstellende, modellgestütze Regelung eines Industrieroboters. In: Fortschritte der Robotik, vol. 13. Vieweg-Verlag, Wiesbaden, (in German).

Shaefers, J., Xu, S.J., Darouach, M., 1993. Sensitivity and error analysis of parameter identification for a class of industrial robots. In: Proc. of the IEEE Int. Conference on Systems, Man and Cybernetics, Le Touquet, pp. 195–200.